Quantum Science and Technology

PAPER • **OPEN ACCESS**

Low-lying energy levels of $^{229}Th^{35+}$ and the electronic bridge process

To cite this article: S G Porsev *et al* 2021 *Quantum Sci. Technol.* **6** 034014

Quantum Science and Technology

PAPER

Low-lying energy levels of $^{229}Th^{35+}$ and the electronic bridge process

S G Porsev[1,2,*], C Cheung[1] and M S Safronova[1]

[1] Department of Physics and Astronomy, University of Delaware, Newark, Delaware 19716, United States of America
[2] Petersburg Nuclear Physics Institute of NRC 'Kurchatov Institute', Gatchina, Leningrad district 188300, Russia
[*] Author to whom any correspondence should be addressed.

E-mail: sergey@udel.edu

Keywords: highly charged ion, calculation of energy levels, estimate of the electronic bridge process rate

OPEN ACCESS

RECEIVED
25 April 2021

REVISED
27 May 2021

ACCEPTED FOR PUBLICATION
7 June 2021

PUBLISHED
28 June 2021

Abstract

The nuclear transition between the ground and the low-energy isomeric state in the ^{229}Th nucleus is of interest due to its high sensitivity to a hypothetical temporal variation of the fundamental constants and a possibility to build a very precise nuclear clock, but precise knowledge of the nuclear clock transition frequency is required. In this work, we estimate the probability of an electronic bridge (EB) process in $^{229}Th^{35+}$, allowing to determine the nuclear transition frequency and reduce its uncertainty. Using configuration interaction methods, we calculated energies of the low-lying states of Th^{35+} and determined their uncertainties. Our calculations showed that the transition energy from the $J = 15/2$ state to the ground state, 8.31 eV, is close to the central value of the experimentally determined nuclear isomer energy, 8.19 eV, and practically coincides with the upper edge value, 8.31 eV. It opens new possibilities for a more precise measurement of the nuclear isomer energy using an EB process.

1. Introduction

A specific feature of the ^{229}Th nucleus is that the energy difference between the ground state and the first excited state is only several eV. An existence of such a low-lying level was established more than forty years ago [1], but a precise measurement of the isomeric state energy turned out to be very difficult. In 1994, Helmer and Reich [2] measured this excitation energy (ω_N) to be 3.5 ± 1 eV. In reference [3], it was obtained as 5.5 ± 1.0 eV. The experiments of Beck *et al* [4, 5] gave an even larger value with less error, $\omega_N = 7.8 \pm 0.5$ eV. Finally, in recent experiments of Seiferle *et al* [6] and Sikorsky *et al* [7], the values $\omega_N = 8.28 \pm 0.17$ and $\omega_N = 8.10 \pm 0.17$ eV were obtained. Both these results were used in an analysis carried out in reference [8], yielding the value $\omega_N = 8.19 \pm 0.12$ eV, which is, in fact, the average of the two results. Thus, the current most precise value differs from the result of 1994 by more than two times, but is in a good agreement with the result obtained in reference [5].

The nuclear transition between the ground and the low-energy isomeric state in the ^{229}Th nucleus is of interest due to its high sensitivity to a hypothetical temporal variation of the fundamental constants [9]. For instance, a possible change of ω_N due to a variation of the fine structure constant α is given by $\delta\omega_N/\omega_N = K\delta\alpha/\alpha$. In reference [10], the sensitivity coefficient K was predicted to be as large as 8200. Local Lorentz invariance violating and Einstein equivalence principle violating effects are also strongly enhanced in the nuclear transition in the ^{229}Th nucleus [11]. Another unique feature of this transition is a possibility to build a very precise nuclear clock [12]. It requires the precise knowledge of the nuclear clock transition frequency and, consequently, further investigations aiming to refine the value of ω_N.

An experimental progress in trapping and sympathetic cooling of highly charged ions (HCIs) (see review in reference [13] for details) using electron-beam ion traps (EBITs) opened new possibilities to use optical transitions of such ions for different applications. As it was discussed in reference [13], an interaction region of an electron beam with maximum magnetic field in EBITs is short enough. It reduces possible electron-beam instabilities and also allows for a high charge density. Both of these effects speed up

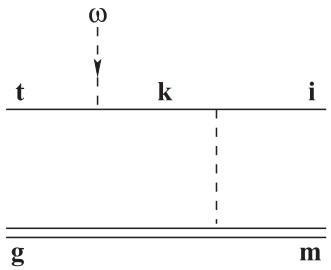

Figure 1. The Feynman diagram of the considered EB process. The single and double solid lines relate to the electronic and the nuclear transitions, correspondingly. The dashed line is the photon line.

the ionization process. If a HCI, considered as a clock candidate, does not have a transition suitable for laser cooling, sympathetic cooling can be done by trapping the HCI together with the cooling ion in the same trapping potential and using their mutual Coulomb interaction. In the recent paper [14], it was suggested to use the electronic bridge (EB) process in Th^{35+} for an accurate determination of the nuclear isomer energy and the energies of the low-lying states, needed to estimate the EB process rate, were calculated.

Since the EB process rate depends drastically on the energies of the states involved in this process, we calculated the energies of the low-lying states of Th^{35+} in different approximations of increasing complexity. The main configuration of the ground state of the ion is $(1s^2, \ldots, 4d^{10}4f^9)$ and we used configuration interaction (CI) method for calculations. First, we performed a nine-electron CI calculation, including nine $4f$ electrons in the valence field while treating all other electrons as the core electrons. Then, we carried out 19- and 25-electron CI calculations, including the $4f, 4d$ and $4f, 4d, 4p$ electrons into the valence field, respectively. In such a way, we were able to estimate the role of core–valence correlations, which allowed us to determine the uncertainties of the energies.

To carry out these calculations for such a complicated open-shell system as Th^{35+}, we used a new parallel atomic structure code package developed and described in reference [15]. This package (i) allows us much quicker computations and (ii) enables us to work with a CI space of a much larger size than was possible previously when we used serial versions of the programs. Using a parallel version of the program for the CI calculation, we were able to use several hundreds of processors simultaneously and, consequently, to work with a large CI space, involving up to 120 millions of determinants.

Using the energies obtained and assuming a resonant character of the induced EB process, we estimated its rate for several possible values of the nuclear isomeric energy. Based on these calculations, we conclude that modern facilities of EBITs and available ultra-violet lasers allow us to determine more precisely the nuclear isomeric energy and reduce its uncertainty.

2. EB excitation

Here we consider the process of the excitation of the nucleus from the ground (g) to the isomeric state (m) by an EB process driven by a one-photon excitation of the electron shell. Such a process, relying on the absorption of an incident photon, can be represented by the Feynman diagram in figure 1. In this process, the electronic shell is promoted by a laser photon from its initial state t to an excited state k and then decays to a lower-lying state i. The energy transferred to the nucleus is used to excite it from the ground to isomeric state. Assuming a resonant character of the process, we take into account only one Feynman diagram that gives the main contribution to the probability of the process.

In the following, we use the formalism developed in references [16–18], with the difference that an $M1$ photon (instead of a $E1$ photon) is absorbed by the electron shell. Such a photon is described by the magnetic moment operator

$$\boldsymbol{\mu} = -\mu_0(\mathbf{J} + \mathbf{S}). \tag{1}$$

Here $\mathbf{J}$ and $\mathbf{S}$ are the total and spin momentum operators and μ_0 is the Bohr magneton determined as $\mu_0 = |e|\hbar/(2mc)$, where e and m is the electron charge and mass, c is the speed of light, and $\hbar$ is the Plank constant. (If not stated otherwise the atomic units $\hbar = m = |e| = 1$ and $c \approx 137$ are used in the following).

We assume that the incident radiation with spectral intensity I_ω is isotropic and unpolarized. Following reference [19] the relation between the EB excitation rate, $\Gamma_{\rm exc}$, and the rate of the inverse spontaneous EB process, Γ, that can be formally described by the mirror-image of figure 1 with an outgoing photon arrow,

can be written as

$$\Gamma_{\rm exc} = \Gamma \frac{4\pi^3 c^2}{\omega^3} g_r I_\omega, \tag{2}$$

where ω is the frequency of the absorbed photon. The factor $g_r \equiv (2I_m+1)(2J_i+1)/[(2I_g+1)(2J_t+1)]$ appears because we average over the initial projections and summing over the final projections of the electronic and nuclear total angular momenta. Here I_m (I_g) is the nuclear spin of the isomeric (ground) state and J_i (J_t) is the total angular momentum of the initial (final) electronic state in the spontaneous EB process.

The general expression for the probability of the EB process was derived in reference [17]. Assuming a resonance character of the spontaneous EB process, its transition rate can be written as,

$$\Gamma \approx \frac{16\pi}{3(2J_i+1)} \left(\frac{\omega}{c}\right)^3 \sum_{K=1}^{2} \frac{B(\tau K) G_K}{(2K+1)^2}. \tag{3}$$

The reduced probabilities, $B(M1)$ and $B(E2)$, of the nuclear magnetic-dipole and electric-quadrupole $m \to g$ transition are determined as

$$B(\tau K) = \frac{1}{2I_m+1} \frac{2K+1}{4\pi} |\langle I_g \| \mathcal{M}_K \| I_m \rangle|^2, \tag{4}$$

where $\tau \equiv M$ for $K=1$ and $\tau \equiv E$ for $K=2$; $\mathcal{M}_1$ and $\mathcal{M}_2$ are the magnetic-dipole and electric-quadrupole nuclear moment operators, and $|I_g\rangle = 5/2^+\ [633]$ and $|I_m\rangle = 3/2^+\ [631]$ are the ground and isomeric nuclear states, respectively, given in their Nilsson classification.

The explicit expression for the quantity G_K was derived in reference [17], and in our case, is reduced to

$$G_K \approx \frac{1}{2J_k+1} \left| \frac{\langle i \| T_K \| k \rangle \langle k \| \mu \| t \rangle}{E_k - E_i - \omega_{\rm N}} \right|^2, \tag{5}$$

where $|i\rangle$, $|k\rangle$, and $|t\rangle$ are the electronic states, E_k and E_i are the energies of the respective states, and J_k is the electron total angular momentum of the state $|k\rangle$. We assume that there is only one state giving the dominant contribution to G_K, while the contribution of all other intermediate states is negligible, i.e., the state $|k\rangle$ is chosen so that $E_k - E_i \approx \omega_{\rm N}$.

The expressions for the single-electron operators T_1 and T_2 can be written as

$$\begin{aligned} T_{1\lambda}(\mathbf{r}) &= -\frac{i\sqrt{2}\,\boldsymbol{\alpha}\cdot \mathbf{C}^{(0)}_{1\lambda}(\mathbf{n})}{cr^2}, \\ T_{2\lambda}(\mathbf{r}) &= -\frac{C_{2\lambda}(\mathbf{n})}{r^3}, \end{aligned} \tag{6}$$

where $\boldsymbol{\alpha}$ is the Dirac matrix, $\mathbf{n} \equiv \mathbf{r}/r$, and $\mathbf{C}^{(0)}_{K\lambda}$ is a normalized vector spherical harmonic defined by (see, e.g., reference [20])

$$\mathbf{C}^{(0)}_{K\lambda}(\mathbf{n}) = \frac{\mathbf{L}}{\sqrt{K(K+1)}} C_{K\lambda}(\mathbf{n}). \tag{7}$$

Here $\mathbf{L}$ is the orbital angular-momentum operator and $C_{K\lambda}$ is a spherical harmonic given by

$$C_{K\lambda}(\mathbf{n}) = \sqrt{\frac{4\pi}{2K+1}} Y_{K\lambda}(\mathbf{n}). \tag{8}$$

A most accurate determination of the nuclear transition frequency $\omega_{\rm N}$ was recently done in reference [8] to be $\omega_{\rm N} = 8.19(12)$ eV. The authors of reference [14] calculated the low-lying energy levels of Th^{35+} and found the transition frequencies from the low-lying excited states with $J = 13/2$ and $J = 11/2$ to the ground state ($J = 15/2$) to be 8.40 eV (which is close to $\omega_{\rm N}$) and 4.2 eV, respectively. As we discuss in detail below, our calculations give the close values, 8.19 and 4.62 eV.

The state with $J = 11/2$ and $E \approx 4.6$ eV can be used as the initial state in the induced EB process. Applying the designations in figure 1, we have $|t\rangle \equiv |J = 11/2\rangle$, $|k\rangle \equiv |J = 13/2\rangle$, and $|i\rangle \equiv |J = 15/2\rangle$. A scheme of the low-lying electronic and nuclear states, involved in the EB process, is presented in figure 2.

We carried out the calculation of the low-lying states in the framework of the CI method using the program package described in reference [21] and further developed in reference [15]. We included the Breit interaction correction and estimated the core–valence correlations. Our results, discussed in more detail in the following sections, confirmed the main conclusion of reference [14] about a possibility to determine accurately the nuclear isomer energy using the EB process with realistic laser parameters.

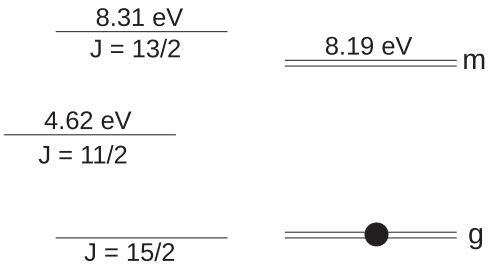

Figure 2. Scheme of the low-lying electronic states (single lines) and the ground and isomeric nuclear states (double lines). The excited states are labeled by energy. The electronic states are additionally labeled by the angular momentum J.

3. Method of calculation and results

We start calculations of energy levels of Th^{35+} belonging to the $(1s^2, \ldots, 4f^9)$ configuration from solutions of the Dirac–Hartree–Fock equations, carrying out a self-consistency procedure for the $[1s^2, \ldots, 4f^9]$ electrons. The Breit interaction was included in this procedure. The remaining virtual orbitals were formed using a recurrent procedure described in [21, 22], where the large component of the radial Dirac bispinor, $f_{n'l'j'}$, was obtained from a previously constructed function f_{nlj} by multiplying it to $r^{l'-l}\sin(kr)$, where l' and l are the orbital quantum numbers of the new and old orbitals ($l' \geqslant l$) and the coefficient k is determined by the properties of the radial grid. The small component $g_{n'l'j'}$ was found from the kinetic balance condition:

$$g_{n'l'j'} = \frac{\boldsymbol{\sigma p}}{2mc} f_{n'l'j'}, \tag{9}$$

where $\boldsymbol{\sigma}$ are the Pauli matrices, $\boldsymbol{p}$ and m are the electron momentum and mass, and c is the speed of light. The newly constructed functions were then orthonormalized with respect to the functions of the same symmetry. In constructing the virtual orbitals, we did not diagonalize the basis set.

In total, the basis set consisted of six partial waves ($l \leqslant 5$), including the orbitals up to 10s, 10p, 10d, 10f, 10g, and 10h. The configuration space grows very rapidly with an increase of the basis set; for this reason the basis set is rather short.

For an accurate calculation of energies, we need to take into account valence–valence and core–valence correlations. The former can be treated explicitly in the framework of the CI method. A CI many-electron wave function of a given angular momentum J and parity can be represented by a linear combination of Slater determinants [23]:

$$\Psi_J = \sum_k a_k \Phi_k. \tag{10}$$

A way to account for core–valence correlations was suggested in reference [23], but in practice, it is applicable when the number of valence electrons does not exceed 4–5. In our consideration, we include nine 4f electrons into the valence field, so such a method is impractical. To estimate the role of different core shells, we carried out several calculations of increasing complexity in the framework of the CI method by sequentially adding the core shells into the valence field. In this way, we carried out the nine-, 19- and 25-electron CI calculations when the 4f, (4f, 4d), and (4f, 4d, 4p), electrons, respectively, were included in the CI space. Below we discuss these calculations in more detail.

3.1. Nine-electron CI

We start from the most simple case of the nine-electron CI. To check the convergence of the CI method, we calculated the low-lying energy levels for five cases. In the first case, we included the single and double excitations of the electrons from the main configuration $4f^9$ to the 6s, 6p, 6d, 6f, 6g and 6h orbitals (we designate it as [6$spdfgh$]). In the other four calculations, we included the single and double excitations to [$nspdfgh$], where $n = 7$–10. We checked that an inclusion of the triple excitations change the energies only by few cm^{-1}. Thus, this contribution can be neglected.

The results are presented in table 1. The terms are determined by their total angular momentum J. The energies of four lowest-lying excited states counted from the ground state and found for different n (when the single and double excitations were allowed to [$nspdfgh$]) are presented in the columns labeled 'E' in cm^{-1}. The energy differences $\Delta(n) \equiv E(nspdfgh) - E(n-1spdfgh)$ and the ratios $\delta_n \equiv \Delta(n)/\Delta(n-1)$ are given in the columns labeled '$\Delta(n)$' (in cm^{-1}) and 'δ_n'. The total values are given in the last row.

To estimate the contribution to the energies from the configurations containing shells with $n > 10$, we note that δ_n for $n = 8, 9, 10$ are numerically close to each other for all terms. Assuming that the same is true

Table 1. Nine-electron CI. The energies of four lowest-lying excited states counted from the ground state and found for different n (when the single and double excitations were allowed to [$nspdfgh$]) are presented in the columns labeled 'E' in cm^{-1}. The energy differences $E(nspdfgh) - E(n-1spdfgh)$ are given in the columns labeled '$\Delta(n)$' (in cm^{-1}). The ratios $\Delta(n)/\Delta(n-1)$ are listed in the columns labeled 'δ_n'. The total values, obtained as $E(n=10)+\Delta(n>10)$, are given in the last row.

	E	$J=9/2$	$\Delta(n)$	δ_n	E	$J=11/2$	$\Delta(n)$	δ_n	E	$J=3/2$	$\Delta(n)$	δ_n	E	$J=13/2$	$\Delta(n)$	δ_n
$n=6$	30 503				36 728				55 006				67 200			
$n=7$	30 279		−224		36 411		−316		54 441		−565		67 255		54.6	
$n=8$	30 171		−108	0.483	36 266		−145	0.459	54 175		−266	0.471	67 290		35.6	0.652
$n=9$	30 118		−52.8	0.487	36 205		−61.2	0.421	54 061		−114	0.430	67 313		23.1	0.648
$n=10$	30 090		−28.0	0.529	36 178		−26.4	0.432	54 010		−51.1	0.447	67 329		15.9	0.689
q[a]				0.500				0.437				0.449				0.663
$n>10$[b]			−35				−13				−29				33	
Total	30 055				36 165				53 980				67 362			

[a] See explanation in the text.
[b] The contribution to the energies from the configurations containing shells with $n>10$.

and for $n>10$ we are able to use the formula for a geometric progression to estimate the respective contribution.

Putting the first term of the geometric progression to be $b_1 \equiv \Delta(7)$, determining q as an average over δ_n for $n=8,9,10$, i.e., $q \equiv (\delta_8+\delta_9+\delta_{10})/3$, and using the equation for the sum of k terms in the geometric progression,

$$S_k = \frac{b_1(1-q^k)}{1-q}, \tag{11}$$

we are able to calculate S_k for any k. Then we can estimate $\Delta(n>10)$, as

$$\Delta(n>10) \approx S_k - (\Delta_8+\Delta_9+\Delta_{10}). \tag{12}$$

For instance, for the $J=9/2$ term we have $b_1 = -224$ cm^{-1}, $q=0.50$, and putting k to be equal to 100, we find $S_{100} \approx -448$ cm^{-1} and $\Delta(n>10) \approx -35$ cm^{-1}. Carrying out similar calculations for other terms, we find the values listed in the row labeled '$n>10$' of table 1. The total values, obtained as $E(n=10)+\Delta(n>10)$, are given in the last row of the table.

3.2. Core–valence correlations

Due to the large number of the valence electrons, we were unable to apply the method combining the CI with a many-body perturbation theory over residual Coulomb interaction [23] or with linearized coupled-cluster method [24] to find the core–valence correlations. To estimate this contribution to the energies, we additionally performed the 19- and 25-electron CI calculations, including the $4d$ and $4d,4p$ electrons into the valence field. In both cases, we allowed the single and double excitations of the electrons from the all valence shells of the main configuration to [$7spdfgh$]. For example, for the $4d^{10}4f^9$ main configuration, the single and double excitations were allowed from the $4d$ and $4f$ shells. We restricted ourselves to the calculation for [$7spdfgh$] because the set of configurations is sufficiently complete in this case and, on the other hand, such a calculation is not extremely demanding in computer resources, even for the case of the 25-electron CI.

We focus on computing the energies of the $J=11/2$ and $J=13/2$ states that are most important for an accurate calculation of the probability of the EB process, as we discussed in section 3. Additionally, if we are interested in only in the states with a large J, it facilitates the CI calculation because it allows us to deal with the CI space of a smaller size. The calculation results of the transition energies obtained for these states in the framework of nine-, 19-, and 25-electron CI calculations, with the excitations allowed to [$7spdfg$], are presented in table 2. The main configurations of the valence electrons are given in the first column. The energies of the excited states, counted from the ground state energy, are given in the columns labeled 'E' (in cm^{-1}). The differences $\Delta(4d^{10}4f^9) \equiv E(4d^{10}4f^9) - E(4f^9)$ and $\Delta(4p^64d^{10}4f^9) \equiv E(4p^64d^{10}4f^9) - E(4d^{10}4f^9)$ are given for each state in the column labeled 'Δ' in cm^{-1}. The sum $\Delta(4d^{10}4f^9) + \Delta(4p^64d^{10}4f^9)$ (we designate it as $\Delta_{\rm Total}$) is presented in the row labeled 'Total'.

Using the values of the energies from tables 1 and 2, we are able to determine the final value of the energies for the $J=11/2$ and $J=13/2$ terms as the sum of the 'Total' value given in table 1 and $\Delta_{\rm Total}$ from table 2. Thus, we finally obtain $E_{J=11/2} \approx 37\,240\ (980)$ cm$^{-1} \approx 4.62(12)$ eV and $E_{J=13/2} \approx 67\,000\ (315)$ cm$^{-1} \approx 8.307(39)$ eV.

Table 2. The energies obtained in the framework of nine-, 19-, and 25-electron CI calculations with the excitations allowed to [7*spdfgh*], are presented. The main configurations of the valence electrons are given in the first column. The energies of the excited states, counted from the ground state energy, are given in the columns labeled 'E' (in cm^{-1}). The differences $E(4d^{10}4f^{9}) - E(4f^{9})$ and $E(4p^{6}4d^{10}4f^{9}) - E(4d^{10}4f^{9})$ are given for each state in the column labeled 'Δ' in cm^{-1}. The sum $\Delta(4d^{10}4f^{9}) + \Delta(4p^{6}4d^{10}4f^{9})$ is presented in the row labeled 'Total'.

	$J = 11/2$		$J = 13/2$	
	E	Δ	E	Δ
$4f^{9}$	36 411		67 255	
$4d^{10}4f^{9}$	37 400	989	66 948	−307
$4p^{6}4d^{10}4f^{9}$	37 487	87	66 899	−49
Total		1076		−356

The uncertainties are mostly determined by the core–valence correlations not taken into account in our consideration. To estimate them, we note that $\Delta(4d^{10}4f^{9})$ is an order of magnitude smaller than $\Delta(4p^{6}4d^{10}4f^{9})$. We assume that a possible contribution from the [1*s*–4*s*] core shells to the energies does not exceed $\Delta(4d^{10}4f^{9})$ and we estimate the uncertainty of the energy as $|\Delta(4d^{10}4f^{9})|$.

Our final values for $E_{J\,=\,11/2}$ and $E_{J\,=\,13/2}$ can be compared with the results obtained in reference [14] to be 4.19 and 8.40 eV, respectively. For instance, for the $J = 11/2$ state, our value, 4.62 eV, differs from the result obtained in reference [14] by 0.41 eV. A half of this difference (0.2 eV) is attributed to the Breit correction, omitted in reference [14], whereas the remaining difference, 0.21 eV, might be explained by a more complete inclusion of the valence–valence and core–valence correlations. In particular, when including the 4*d* shell into the valence field, the authors of reference [14] were obliged to reduce the configuration space (due to limitations of the computing facilities), disregarding certain double-electron excitations from the 4*d* shell to the virtual orbitals.

3.3. EB process excitation rate

Using equations (2)–(5), we are able to estimate the EB process probability. To find the probability of the spontaneous process given by equation (3) we need to calculate the matrix elements of the operators T_1, T_2, and μ in equation (5).

We carried out this calculation for the largest 25-electron CI when single and double excitations were allowed to [7*spdfgh*] and obtained

$$\begin{aligned} |\langle J = 15/2 \| T_1 \| J = 13/2 \rangle| &\approx 2.0 \text{ a.u.}, \\ |\langle J = 15/2 \| T_2 \| J = 13/2 \rangle| &\approx 39 \text{ a.u.}, \\ |\langle J = 13/2 \| \mu \| J = 11/2 \rangle| &\approx 2.28 \mu_0. \end{aligned} \tag{13}$$

The calculation performed in the framework of the nine-electron CI with allowing single and double excitations to [10*spdfgh*] led to the values that differ by less than 1% from the results given above.

The values of the reduced probabilities, $B(M1)$ and $B(E2)$, of the nuclear $m \to g$ transition available in the literature are contradictory. In reference [25], the value of $B(M1)$ was found to be 0.048 Weisskopf units (W.u.). The calculation of Ruchowska *et al* [26] led to the value 0.014 W.u., while the recent model calculation of Minkov and Pálffy [27] predicted the $B(M1)$ value in the limits of 0.005–0.008 W.u., an order of magnitude smaller than the result reported in reference [25].

A similar situation arises for $B(E2)$. Strizhov and Tkalya [28], referring to reference [29], cited the value of several W.u., while in reference [27], it was found an order of magnitude larger value, in the limits of 29–43 W.u..

We note that in references [16–18], the values $B(M1) = 0.048$ W.u. [25] and $B(E2) \sim 1$ W.u. [28, 29] were used for the calculation. As a result, the contribution of the $E2$ channel was small and this channel was disregarded. In this work, we use for an estimate of the EB transition rate the recent values, $B(M1) = 0.005$ W.u. and $B(E2) = 29$ W.u., obtained in reference [27]. In this case the $E2$ channel should be included into consideration.

Table 3. Possible values of the nuclear transition frequency ω_N are listed in the first column. The quantities G_1, G_2, and Γ are given by equations (5) and (3). The values of the EB excitation rate, Γ_{exc}, are presented in the fifth column.

ω_N(eV)	G_1(a.u.)	G_2(a.u.)	$\Gamma(s^{-1})$	$\Gamma_{exc}(s^{-1})$
8.31	1570	5.93×10^5	5.70×10^{-4}	0.3
8.19	1.1	404	3.50×10^{-7}	2.10×10^{-4}
8.07	0.3	99	7.70×10^{-8}	5.0×10^{-5}

For the $M1$ and $E2$ transitions rates from the nuclear excited state to the ground state, Weisskopf units can be expressed in usual units as

$$M1\text{: } 1 \text{ W.u.} = 1.790\left(\frac{e\hbar}{2m_p c}\right)^2, \qquad E2\text{: } 1 \text{ W.u.} = 5.940 \times 10^{-6} A^{4/3} (eb)^2, \tag{14}$$

where m_p is the proton mass and A is the number of nucleons in the nucleus. Using these definitions, we can express $B(M1)$ and $B(E2)$ in a.u. as $B(M1) \approx 3.5 \times 10^{-14}$a.u. and $B(E2) \approx 3.1 \times 10^{-16}$a.u.

As follows from equations (3)–(5), the EB transition rate depends substantially from the magnitude of the nuclear transition frequency ω_N determined as 8.19(12) eV in reference [8]. To illustrate it we calculated these rates for three values of ω_N: its central value 8.19 eV and two edge values of the uncertainty interval 8.31 and 8.07 eV. We note that the frequency of the absorbed photon ω is determined as $\omega = \omega_N - E_{J=11/2}$ and assume that the time-averaged spectral intensity is $I_\omega \simeq 10^{-3}$(W m^{-2}) s [14, 16].

The results are presented in table 3. The possible values of the nuclear transition frequency ω_N are listed in the first column. The quantities G_1, G_2, and Γ, given by equations (5) and (3), are listed in columns 2–4. We note that for the used values of $B(M1)$ and $B(E2)$, both terms in equation (3) give approximately the same contribution. The values of the EB excitation rate per ion, Γ_{exc}, are presented in the fifth column for different ω_N.

As seen from table 3, the largest Γ_{exc}, obtained in the case of $\omega_N = 8.31$ eV, reaches 0.3 s^{-1}. This is due to this value of ω_N being very close to $E_{J=13/2} \approx 8.307$ eV, leading to a very small denominator in equation (5) and, respectively, very large $G_{1,2}$ and Γ_{exc}. For the other two considered values of the nuclear transition frequency, 8.19 and 8.07 eV, there is no such a resonant enhancement of the effect and the EB excitation rates are several orders of magnitude smaller. Our results are in a reasonable agreement with those obtained in reference [14].

4. Conclusion

We carried out the calculation of the low-lying energy levels for such a complicated multivalent ion as Th^{35+}. To determine the contribution of the valence–valence and core–valence correlations, we performed the nine-, 19-, and 25-electron CI calculations, including $4f$, $4f, 4d$, and $4f, 4d, 4p$ shells, respectively, into the valence field. Our calculation showed that the transition energy from the $J = 15/2$ state to the ground state, 8.31 eV, is close to the central value of the experimentally determined nuclear isomer energy, 8.19 eV, and practically coincides with the upper edge value, 8.31 eV. It opens new possibilities for a more precise measurement of the nuclear isomer energy using an EB process.

We studied an EB process scheme and estimated the excitation rates of the spontaneous and (inverse) induced EB processes for possible values of the $g \to m$ nuclear transition frequency ω_N. We found the EB excitation rate per ion to be 0.3 s^{-1} in the case of $\omega_N = 8.31$ eV. For other considered values of the nuclear transition frequency, 8.19 and 8.07 eV, this rate is 3–4 orders of magnitude smaller. Based on these results and on the study of reference [14] where typical EBIT conditions were considered, we conclude that an efficient population of the nuclear isomer state and a precise determination of its energy using an EBIT and available ultra-violet lasers is already attainable. The Th^{35+} ion is a very promising candidate for such an experiment.

Acknowledgments

We are grateful to P Bilous and A Pálffy for valuable discussion and useful remarks. This work is a part of the 'Thorium Nuclear Clock' project that has received funding from the European Research Council (ERC)

under the European Union's Horizon 2020 research and innovation program (Grant Agreement No. 856415). SP acknowledges support by the Russian Science Foundation under Grant No. 19-12-00157. This research was supported in part through the use of the Caviness community cluster at the University of Delaware.

Data availability statement

The data that support the findings of this study are available upon reasonable request from the authors.

ORCID iDs

S G Porsev https://orcid.org/0000-0003-0417-2726
M S Safronova https://orcid.org/0000-0002-1305-4011

References

[1] Kroger L A and Reich C W 1976 *Nucl. Phys.* A **259** 29
[2] Helmer R G and Reich C W 1994 *Phys. Rev.* C **49** 1845
[3] Guimarães -Filho Z O and Helene O 2005 *Phys. Rev.* C **71** 044303
[4] Beck B R, Becker J A, Beiersdorfer P, Brown G V, Moody K J, Wilhelmy J B, Porter F S, Kilbourne C A and Kelley R L 2007 *Phys. Rev. Lett.* **98** 142501
[5] Beck B R *et al* 2009 Improved value for the energy splitting of the ground-state doublet in the nucleus ^{229m}Th *Technical Report No. LLNL-PROC-415170* Lawrence Livermore National Laboratory
[6] Seiferle B *et al* 2019 *Nature* **573** 243
[7] Sikorsky T *et al* 2020 *Phys. Rev. Lett.* **125** 142503
[8] Peik E, Schumm T, Safronova M S, Pálffy A, Weitenberg J and Thirolf P G 2021 *Quantum Sci. Technol.* **6** 034002
[9] Flambaum V V 2006 *Phys. Rev. Lett.* **97** 092502
[10] Fadeev P, Berengut J C and Flambaum V V 2020 *Phys. Rev.* A **102** 052833
[11] Flambaum V V 2016 *Phys. Rev. Lett.* **117** 072501
[12] Peik E and Tamm C 2003 *Europhys. Lett.* **61** 181
[13] Kozlov M G, Safronova M S, Crespo López-Urrutia J R and Schmidt P O 2018 *Rev. Mod. Phys.* **90** 045005
[14] Bilous P V, Bekker H, Berengut J C, Seiferle B, von der Wense L, Thirolf P G, Pfeifer T, López-Urrutia J R C and Pálffy A 2020 *Phys. Rev. Lett.* **124** 192502
[15] Cheung C, Safronova M and Porsev S 2021 *Symmetry* **13** 621
[16] Porsev S G, Flambaum V V, Peik E and Tamm C 2010 *Phys. Rev. Lett.* **105** 182501
[17] Porsev S G and Flambaum V V 2010 *Phys. Rev.* A **81** 032504
[18] Porsev S G and Flambaum V V 2010 *Phys. Rev.* A **81** 042516
[19] Sobelman I I 1979 *Atomic Spectra and Radiative Transitions* (Berlin: Springer)
[20] Varshalovich D A, Moskalev A N and Khersonskii V K 1988 *Quantum Theory of Angular Momentum* (Singapore: World Scientific)
[21] Kozlov M G, Porsev S G, Safronova M S and Tupitsyn I I 2015 *Comput. Phys. Commun.* **195** 199
[22] Kozlov M G, Porsev S G and Flambaum V V 1996 *J. Phys. B: At. Mol. Opt. Phys.* **29** 689
[23] Dzuba V A, Flambaum V V and Kozlov M G 1996 *Phys. Rev.* A **54** 3948
[24] Safronova M S, Kozlov M G, Johnson W R and Jiang D 2009 *Phys. Rev.* A **80** 012516
[25] Dykhne A M and Tkalya E V 1998 *Pis'ma Zh. Eksp. Teor. Fiz.* **67** 233
Dykhne A M and Tkalya E V 1998 *JETP Lett.* **67** 251
[26] Ruchowska E *et al* 2006 *Phys. Rev.* C **73** 044326
[27] Minkov N and Pálffy A 2019 *Phys. Rev. Lett.* **122** 162502
[28] Strizhov V F and Tkalya E V 1991 *Zh. Eksp. Teor. Fiz.* **99** 697
Strizhov V F and Tkalya E V 1991 *Sov. Phys.-JETP* **72** 387
[29] Bemis C E, McGowan F K, Ford J L C, Milner W T, Robinson R L, Stelson P H, Leander G A and Reich C W 1988 *Phys. Scr.* **38** 657